

FORMATION OF CHROMOSPHERIC RESONANCE LINE PROFILES IN SUPERGIANTS

GIBOR S. BASRI

Joint Institute for Laboratory Astrophysics, University of Colorado and National Bureau of Standards

Received 1979 December 3

ABSTRACT

The formation of chromospheric resonance line profiles is examined for the case of the relatively low-density atmospheres appropriate to late-type supergiants. The effects of partial frequency redistribution control the emergent line profiles, to the extent that even an isothermal atmosphere can give rise to apparent emission features. Schematic model chromospheres are used to demonstrate the effects of different velocity fields and temperature-density structures on the line profiles, as a first step toward a clearer understanding of the chromospheric line profiles and why supergiants have broad emission lines (the Wilson-Bappu effect). Neither the Doppler nor the mass column density explanation alone can explain the Wilson-Bappu effect in supergiants, but both theories may play a role.

Subject headings: line formation — stars: chromospheres — stars: supergiants

I. INTRODUCTION

Self-reversed emission features found in the resonance lines of Ca II and Mg II have served as the primary diagnostics of stellar chromospheres. They are important because they are sensitive to the temperature and density distributions in stellar chromospheres, and through the well-known Wilson-Bappu effect they serve as indicators of stellar distance and absolute luminosity. The cores and inner wings of these lines have been employed to obtain semiempirical models of the density and temperature structure of specific stellar chromospheres. It is important, therefore, to understand how these line profiles are formed, given a model chromosphere, if we are to invert the profiles to calculate chromospheric densities, temperatures, and velocity fields and to understand the Wilson-Bappu effect.

Because these are resonance transitions, it was realized a few years ago that complete frequency redistribution is not an accurate description of the radiative transfer in both the line core and wings. Owing to the sharpness of the ground state, the scattering in the wings (beyond the point where Doppler motions can readily redistribute photons in frequency) should be nearly coherent unless the atom suffers a collision while in the excited state. This partial coherency in the wings leads to a frequency-dependent source function and to a different line profile for a given atmospheric model from that obtained with the complete redistribution (CRD) approximation (Vernazza, Avrett, and Loeser 1973). Milkey and Mihalas (1973) and Shine, Milkey, and Mihalas (1975) showed that for the solar chromosphere a partial redistribution (PRD) treatment is able to resolve certain discrepancies between observations and CRD line calculations. It was found,

however, that the PRD models require a higher temperature minimum to fit observations than is implied by a continuum model (Ayres and Linsky 1976). Some models have also been constructed using stellar observations of Mg II and Ca II (e.g., Kelch *et al.* 1978), although both the observations and theoretical models to which the method is compared are by nature cruder for these cases than for solar calculations.

A theoretical formulation for partial redistribution in atomic lines has been given by Hummer (1962) and Omont, Smith, and Cooper (1972), and collisional redistribution has been observed experimentally by Carlsten, Szöke, and Raymer (1977), among others. An excellent discussion of line transfer with partial redistribution is given by Mihalas (1978). One can write the redistribution function (which gives the probability of a photon being absorbed at frequency ν and reemitted at ν') as (cf. Milkey and Mihalas 1976)

$$R(\nu, \nu') = (1 - \Lambda) R_{\text{II}}(\nu, \nu') + \Lambda R_{\text{III}}(\nu, \nu');$$

$$\Lambda = \frac{\Gamma_{\text{col}}}{\Gamma_{\text{col}} + \Gamma_{\text{rad}}}.$$

Here Γ_{col} and Γ_{rad} are the collisional and radiative damping parameters for the given transition. Since the functions R_{II} and R_{III} derived by Hummer (1962) are costly to compute, it is convenient to use approximations. Complete redistribution has been shown to be an adequate substitution for R_{III} (Frisch 1979; Vardavas 1976), and this approximation is commonly used. In the partial coherent scattering (PCS) approximation $R_{\text{II}}(\nu, \nu')$ is replaced by $\delta(\nu, \nu')$, and for $\Lambda \ll 1$ each frequency is almost entirely decoupled from all others.

This treatment is not applicable to the Doppler core of the line where Doppler shifts produced by gas motions (either thermal or turbulent) result in complete redistribution. It is desirable to account for the Doppler core without use of the full expression for R_{II} , which can be quite costly to compute. As suggested by Jeffries and White (1960) and modified by Kneer (1975), one can write

$$R_{II}(\nu, \nu') \approx P_\nu \delta(\nu, \nu') + (1 - P_\nu) \phi_\nu \phi_{\nu'},$$

where ϕ is the Voigt function and P_ν is a somewhat arbitrary function that yields pure complete redistribution in the Doppler core, and switches exponentially to coherent scattering in the wings with an e -folding length of a few Doppler widths. This expression defines partial coherent scattering (PCS) in this paper.

When PRD is applicable, the factors controlling the emergent wing intensity profile are primarily $T(\tau)$, $\Lambda(\tau)$, and $r_\nu = K_c/K_{\nu, \text{line}}$. This last factor is important when the continuum absorption opacity K_c is an appreciable fraction of $K_{\nu, \text{line}}$, or if the continuum source function is very much greater than the line source function. In the core, on the other hand, the primary controlling factors are $T(\tau)$, $v_T(\tau)$, and $\epsilon(\tau)$, where $\epsilon = C_{ul}/A_{ul}$ is the probability of collisional photon destruction rather than scattering. For resonance lines ϵ is usually quite small, with values of 10^{-6} to 10^{-7} for the lines of interest in supergiants. Thus the scattering integral is the dominant term in the line source function.

Supergiants offer an interesting testing ground for PRD radiative transfer because PRD effects are more pronounced in their lower density atmospheres and because the line profiles observed have much broader emission cores than in dwarfs or giants. The explanation of this latter point will shed some light on the physical causes of the Wilson-Bappu effect, i.e., the very tight correlation between stellar absolute luminosity and emission width in chromospheric resonance lines. The traditional explanation for this effect is that the emission feature broadens because the atmospheric turbulence (Doppler velocities) is higher in these stars, but PRD theory has suggested to some authors (see Ayres 1979) that turbulence can only play a secondary role and that the temperature-density structure varies in the manner required to produce this effect. In this paper I examine in detail the formation of line profiles in low-density atmospheres when PRD effects are important, and show that commonly accepted ideas about the line formation do not accurately describe that physical regime. I will discuss some relevant factors that could give rise to the Wilson-Bappu effect in low-gravity stars and the reasons for the observed variation in appearance of emission profiles with stellar gravity.

In § II, I examine the transfer problem in an isothermal atmosphere when the incoherence fraction Λ becomes very small, both for the PCS and full PRD treatments. I show that PCS tends to become a poor approximation as Λ is reduced, and that the emergent line profile can have a self-reversed emission feature

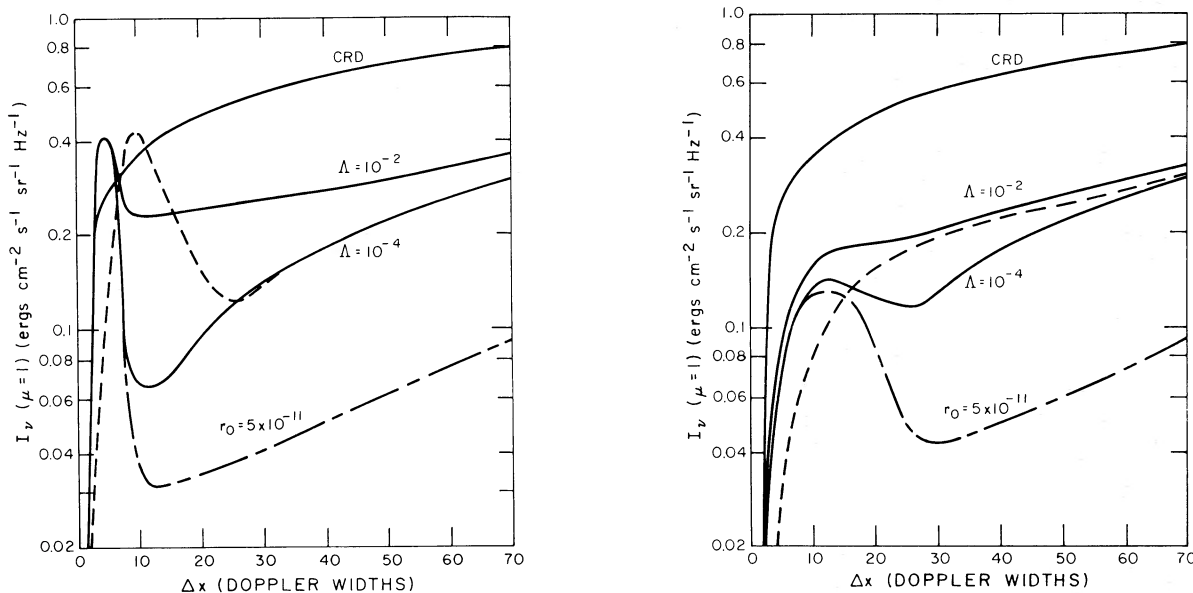


FIG. 1.—(a) The emergent intensity profiles calculated with PCS for an isothermal atmosphere ($B_\nu = 1$) and various values of the coherence fraction Λ . The dashed line shows the profile for $\Lambda = 10^{-4}$ and a gradient in Doppler width from 1 to 4. The dash-dot line shows the effect for $\Lambda = 10^{-4}$ of lowering r_0 from 10^{-9} to 5×10^{-11} . (b) Same as Fig. 1a but for the full partial redistribution treatment. The effects of Doppler diffusion are evident by comparison. The effect of r_0 is also more visible.

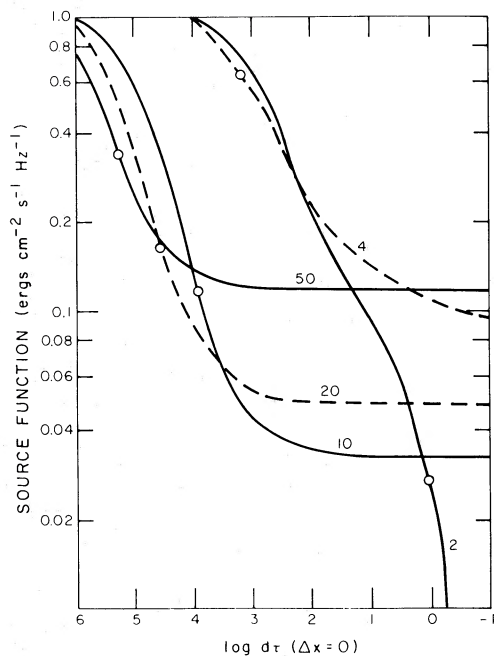


FIG. 2a

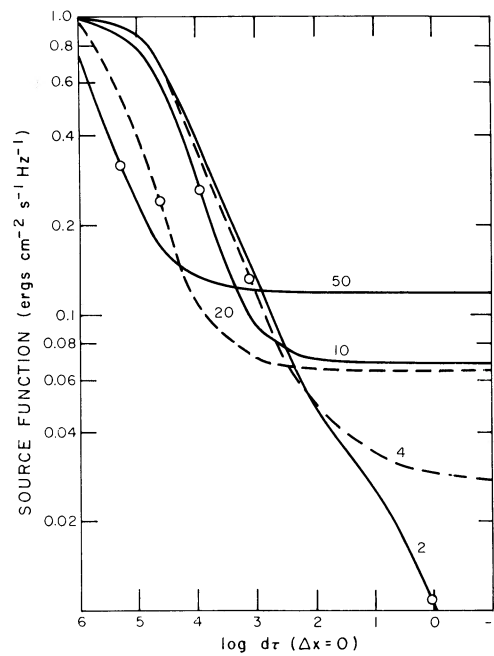


FIG. 2b

FIG. 2.—(a) The frequency dependent source functions for the $\Lambda=10^{-4}$ case of Fig. 1. The numbers indicate the value of Δx to which each source function corresponds, and the circles give the location of $\tau=1$ for each frequency. The formation of the line profile may be traced by following the circles from lower to higher frequencies. (b) Same as Fig. 2a but for the full partial redistribution treatment.

similar to resonance lines formed in a chromosphere even when the atmosphere is isothermal. In § III, I discuss the effects of turbulence of various scales on the line profile, in § IV the effect of the background continuum, and in § V, I study schematic chromospheres having various gravities, turbulent velocities, and values of Λ to explore the possible causes of the Wilson-Bappu effect. The incoherence fraction is discussed in § VI.

II. ISOTHERMAL ATMOSPHERES

The first case I consider is an isothermal atmosphere [$B_v(\tau)=1$] using a Voigt opacity profile with $a=5 \times 10^{-4}$, a constant Doppler width, thermalization parameter $\epsilon=5 \times 10^{-6}$, and continuum to line center opacity ratio $r_0=1 \times 10^{-9}$. Although I find the PCS treatment to be too inaccurate for stellar modeling, I present results from it first because they are more illustrative of the effects I wish to demonstrate. Emergent-intensity profiles at $\mu=1$ using the PCS formulation are shown in Figure 1a for a series of identical calculations in which only Λ is varied from 10^{-4} to 1 (CRD). Notice that for the smaller value of Λ , the emergent profile looks very much like the usual chromospheric emission line profile, with a central minimum, emission peak, and second minimum beyond the emission feature which might normally be ascribed to the location of a temperature minimum at $\tau=1$ at the wavelength of the

minimum. The profile becomes a simple absorption line as CRD is approached ($\Lambda \rightarrow 1$). This behavior can be understood by examining the optical depth dependence of the frequency dependent source functions, as shown in Figure 2a for the $\Lambda=10^{-4}$ case.

This sort of case was first studied by Hummer (1969), who found that an apparent emission feature could be produced in certain cases, and the reader is referred to that paper for a more detailed explanation of how the effect arises. Hummer did not, however, include a background continuum or make the analogy to observed chromospheric profiles.

As one moves away from the Doppler core, the source functions tend toward the monochromatic scattering form appropriate for each monochromatic optical-depth scale outside the Doppler core. These source functions rapidly decouple from the line-center source function and B_v , so that the emergent intensity drops as Δx increases. The sharpness of this drop is controlled by the extent to which coherent scattering becomes dominant, which for PCS is determined by the value of P_v in the Kneer weights. The intensity then rises again as the background continuum term in the source function becomes dominant far out in the wings. The intensity would level off when $P_v \approx 1$ if there were no continuum opacity, because $S_v(\tau_v)$ is constant (appropriate to coherent scattering) in an isothermal atmosphere. The continuum effects are demonstrated in Figure 1 with $r_0=5 \times 10^{-11}$ and $\Lambda=10^{-4}$.

There are a number of factors which can influence the width of the apparent emission feature. In the simple case discussed above, the position of the “ K_1 minimum” is determined mostly by P_r and to a lesser extent r_r . Thus the emergent profile is largely an expression of the redistribution function, containing very little information on the thermal structure of the atmosphere. The emission feature broadens in $\Delta\lambda$ when the Doppler width is increased, and broadening in Δx can be produced by gradients in the Doppler width as can be seen in Figure 1. Temperature gradients are an added complication; a steep temperature gradient sufficiently deep in the atmosphere can cause the emission feature to broaden because monochromatic source functions further out in the wings will respond to the temperature rise.

The primary physical process ignored by use of the PCS treatment is that Doppler shifting is not confined to the Doppler core; that is, a photon in the wing can be shifted within three Doppler widths of its initial frequency just as in the core. The real PRD weights are delta functions convolved with a Maxwellian velocity distribution. Thus each frequency point in the wings communicates with adjacent frequency points, and “Doppler diffusion” of photons far into the wings can occur after many scatterings of a core photon. The importance of this process depends on the likelihood of its occurrence compared to other processes such as collisional redistribution or true absorption. When both ϵ and $\Lambda \ll 1$, Doppler diffusion can be important. To study Doppler diffusion, I used the correct redistribution weights, Hummer’s $R_{II}(\nu, \nu')$, but this is computationally expensive. To allow for Doppler diffusion, the frequency quadrature must also have spacings of $\Delta x < 3$ everywhere. I used an interpolation scheme to reduce the computations required, but the calculation of the weights still required as much computer time as the entire radiative-transfer calculation, instead of being a small fraction of it as with the Kneer approximation. The effects of Doppler diffusion are substantial, as shown in Figure 1*b*, in which the same cases as in Figure 1*a* are plotted except for the treatment of the weights. Notice that Doppler diffusion causes the width of the emission feature to increase, but largely fills in the “ K_1 minimum” for the cases shown. The minimum reappears when a temperature gradient is included as will be shown in the next section (even without a temperature minimum) for the reasons discussed above, or when r_0 is reduced (see Fig. 1*b*). *This test shows the importance of treating the weights correctly for very coherent cases.* I found that in realistic chromospheric models for supergiants the use of PCS always introduced an artificial K_1 minimum feature at small $\Delta\lambda$ compared to the correct result obtained using PRD, thus leading to emission features that always are too narrow. This effect is apparent in comparing the $r_0 = 5$

$\times 10^{-11}$ cases for PCS and PRD. In Figure 2*b* the source functions analogous to Figure 2*a* are plotted. The effect of PRD is to reduce the coupling of the monochromatic source functions near the line center to the Planck function, but to increase the coupling somewhat in the wings because of the leakage of radiation outward from line center.

The main point of this section is that partial coherency effects can lead to an apparent emission feature even when there is no temperature rise in an atmosphere, and that there need be no temperature minimum to produce a “ K_1 minimum” in a resonance line profile. These effects arise when there is great coherency in the line wing and not in the line core, as is typically the case for strong resonance lines in supergiants. I do not mean to suggest that cool supergiants do not have chromospheres, but have tried to show that the sensitivity of their resonance line profiles to the thermal structure of the atmosphere is greatly reduced. Vardavas and Cannon (1976) and Rutten and Milkey (1979) have discussed other cases in which PRD effects can lead to unexpected emission features. It is clear that caution must be exercised in the interpretation of line profiles when PRD effects are very important; the line formation problem can often lead to counterintuitive effects.

III. VELOCITY FIELDS

I now consider the effects of turbulence of various scales on the line profile. In the microturbulent limit, gas motions are assumed to occur on scales small compared with a photon mean free path, such that the net effect is to increase the Doppler-width parameter for the line above its thermal value. Values for stellar microturbulence have traditionally been found from curve-of-growth analyses, and in the Sun even spatially resolved profiles show nonthermal broadening. Solar microturbulence values range from 1 km s^{-1} in the photosphere to over 10 km s^{-1} at the transition region. Since this method often results in supersonic values in supergiants, there is some doubt whether this method actually measures turbulent motions. In the macro-turbulent limit, widely separated large-scale elements on a stellar surface have different velocities and independently formed line profiles. In this approximation a Gaussian smearing function is applied to a static computed profile to simulate the effects of averaging. Both forms of turbulence have been used to help match theoretical profiles computed for static atmospheres to observed ones. There should also be turbulence or waves on intermediate scales, where the details of the velocity field must be treated explicitly in the line transfer calculation. Using angle-averaged redistribution functions for PRD computations requires solving the transfer equation in the comoving fluid frame at each depth (cf. Magnan 1974).

The case of a gradient in the Doppler width is shown by the dashed curves on Figures 1a and 1b for the same isothermal atmosphere. The Doppler width increases from the bottom to the top by a factor of 4 (linearly in $\log \tau$) for these cases, a situation not dissimilar from the Sun. The position of the “K₁ minimum” is moved outward in Δx for the PCS computation, and a similar effect is seen for the PRD computation when there is also a temperature gradient. For the isothermal PRD case, the minimum is filled in. It seems that traditional explanations of the Wilson-Bappu effect based on turbulence could have some merit, because it is able to broaden emission features despite the fact that the minimum feature is formed well outside the Doppler core ($\Delta x \lesssim 3$). This effect occurs largely because of Doppler diffusion and the fact that the emission core can extend well beyond the Doppler core. The emission feature arises because of a partial coupling of the line source function to the Planck function; the behavior and extent of the emission feature can be controlled by changes in both the Planck function and the extent of coupling to it. If the Doppler width increases, the coupling range of frequency points outside the Doppler core is increased independently of their distance from line center. In this manner the effect of turbulent velocities can be felt well outside the Doppler core, although the actual width of the emission feature is a result of a combination of many factors.

Of course, the emission feature can be broadened in $\Delta \lambda$ merely by increasing Doppler microturbulent velocities even without a gradient (which changes the Δx to $\Delta \lambda$ conversion factor), but for supergiants this requires extremely large velocities. Macroturbulent broadening is not very attractive either, because it will fill in the central reversal quite readily if much broadening of the feature is required; this is a result of its application *after* the intrinsic profile is computed.

To study more carefully the effects of microscale and mesoscale turbulence, I used a schematic atmosphere consisting of a monotonically increasing temperature and applied the PRD analysis in the comoving frame, using a code developed by Mihalas *et al.* (1976). The two-level model atom was chosen to represent Mg II in a star with $\log g = 1.35$. Atomic parameters were from Shine (1975*b*). More details of these calculations can be found in Basri (1979). First a profile was calculated without any velocity fields at all (except for thermal broadening) to serve as a comparison standard. The profile has narrow emission peaks and a deep, narrow central reversal as shown in Figure 3. With the addition of a microturbulent velocity of three fiducial Doppler widths everywhere, the central reversal becomes much broader, and the emission peaks move out to three times their former value in Δx as expected. The important thing is that the resultant profile has a very

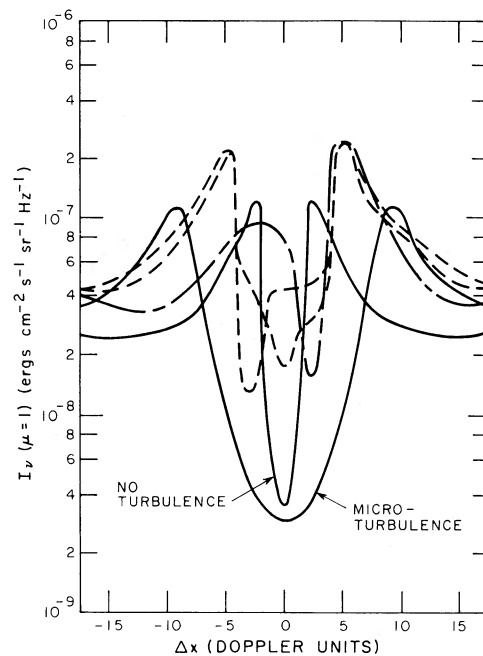


FIG. 3.—Emergent profiles for an atmosphere with temperature increasing outward. *Solid lines*, the profiles for a completely static atmosphere and with microturbulence of three Doppler widths. *Dashed lines*, the profiles for a case with no microturbulence and sinusoidal waves of wavelength 4×10^5 km and amplitude three Doppler widths at two phases separated by $\pi/2$. *Dash-dot line*, the profile for a wavelength of 16×10^5 km showing a marked asymmetry in the emission peak intensities.

broad and deep central reversal compared to the positions of the peaks, and is therefore qualitatively different from observed stellar profiles. Macroturbulence applied to this profile will tend to wash out the emission peaks before having a noticeable effect on the position of the minima.

The question of mesoscale velocities is more complex, and the results I report are only schematic and indicative of possible trends. I used the same atmosphere as above with zero microturbulence, and imposed sinusoidal waves on it with a velocity amplitude of three fiducial Doppler widths. The sinusoidal variation is taken to be geometric; that is, with a given wavelength relative to the geometrical height scale of the chromosphere, which is established using hydrostatic equilibrium for the given gravity. In this case the height of the chromosphere is 1.9×10^6 km, which is thin compared to a typical stellar radius for a supergiant of this gravity. My goal was to find the maximum wavelength that did not produce gross asymmetries in the emergent emission peaks; such a velocity field could masquerade as “turbulence” even in a one-component model. Asymmetries would normally be interpreted as macroscopic velocity gradients in the atmosphere (e.g., Chiu *et al.* 1975). Of course if there

are waves of different phases on the stellar surface, the flux profile might still be symmetric, but I am looking for the case in which the intrinsic intensity profiles are symmetric (discarding the averaging in the former case as a form of macroturbulence).

Tests were made with wavelengths of 2, 4, 8, and 16×10^5 km. I found that even with wavelengths of 8×10^5 km, which is almost half of the total chromospheric extent, the emission peaks remained almost symmetric. This is because the velocity field changes sufficiently rapidly over the (scattering) region of formation of the emission peaks compared to the line core that no sustained effect on them is built up by shifts of the core. The profile has some qualitative changes from the microturbulent case, however, which bring it into better agreement with observations (see Fig. 3). Even after averaging over phases, the central reversal is little more than half as wide and almost 10 times shallower than the microturbulent case. The depth of the central reversal is then similar to the "K₁" minima as in observations. Nonradial pulsations with $l \approx 10^2 - 10^3$, for example, would suffice to produce these kinds of waves. Although such modes may exist on the Sun (higher orders almost certainly are present), it is speculative to imagine that they occur with the appropriate amplitude on late-type supergiants. Other forms of turbulence, on smaller scales, are at least as plausible; this exercise has been only for the purpose of finding an upper limit to the scale length which yields broadened symmetric line profiles.

It is possible that such mesoscale velocities can help to resolve the long-standing question of why computed line profiles always have deeper central intensities than

observed, even after corrections have been made for instrumental and observational smearing.

This result has been noted by previous authors for the case of complete redistribution. Shine (1975a) studied the effect of time averaging sine and sawtooth waves, and Gail, Sedlmayr, and Traving (1975) and Frisch and Frisch (1976) considered a more statistical form of turbulence with intermediate scale lengths. In all cases they found that the central reversal is less deep for mesoscale velocity fields, for a wide variety of line strengths and with both LTE and non-LTE treatments. These results have obvious implications for any curve-of-growth analysis, and on the attempt to use the residual intensity in strong resonance lines as a diagnostic of nonradiative heating in early type stars. Baliunas *et al.* (1979) have argued that the fact that the chromospheric models of Kelch *et al.* (1978) predict central reversals that are too deep implies that the upper chromospheric pressure must be greater, but the effect of mesoscale velocities is to greatly reduce the usefulness of this diagnostic for determining pressure at all.

IV. THE EFFECT OF THE BACKGROUND CONTINUUM

Although PRD effects are most pronounced for strong resonance lines whose opacity is much greater than the background continuum, the continuum term still plays a surprisingly important role in determining the line profile. As mentioned in § II, the continuum is partly responsible for the "K₁ minimum" feature, and examination of Figure 1 shows that the magnitude of the continuum term has a strong effect on the wing intensity outside the minimum. The continuum term

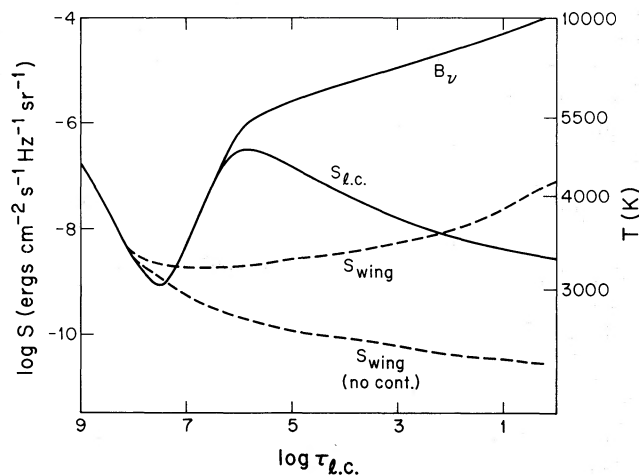


FIG. 4.—Source functions from a supergiant model in Basri (1979) displaying the marked effect that inclusion of a background continuum term has on the line wing. The continuum source function was taken to be B_ν , with $\tau_0 \approx 10^{-9}$ near the temperature minimum increasing to 10^{-6} at the top of the atmosphere. The line center source function is shown, along with source functions at a point in the k line wing ($\Delta\lambda = 2.8$ Å) which becomes optically thin at the temperature minimum.

enters the total source function as a combination of opacity and source factors which are, approximately (cf. Ayres 1976),

$$S_c \sim \frac{K_c B_\nu}{K_0 \phi_\nu b_i}$$

with b_i a possible correction for a non-LTE continuum. This term can have a sizable impact on the total source function for a number of reasons. Although the ratio r_0 is quite small for the cases of interest ($\lesssim 10^{-9}$) near wing optical depth unity, the presence of ϕ_ν in the denominator can make the factor much larger for points in the wing many Doppler widths from line center (where K_1 is located in supergiants). Furthermore, r_0 tends to become larger in the upper chromosphere as the line opacity is diminished by ionization.

The primary reason the term is important is the presence of B_ν as a source term for absorption continua. With a chromospheric temperature rise this term can be many orders of magnitude greater than the pure coherent scattering line source function would be, especially for ultraviolet lines. In Figure 4 is plotted a typical case for Mg II in a late-type supergiant (cf. Basri 1979). For this model, $\Lambda \sim 10^{-4}$ to 10^{-3} and $r_0 \sim 10^{-10}$ to 10^{-9} ; the wing source functions are plotted for a frequency which becomes optically thin at the temperature minimum. The enormous difference between B_ν and the pure line source function is obvious; such an enormous relative term has an effect even at very small wing optical depths. The effect is further enhanced by the strong scattering nature of the source function which allows a deeper penetration of the bright radiation from above. The wing source function is raised significantly everywhere except at depth, and the emergent intensity in the wing is raised significantly. Even if the continuum source function is non-LTE (as with the Balmer continuum for Mg II k), there is still a pronounced effect, although the departure coefficient in the upper chromosphere can reduce its magnitude significantly. Thus it is important to treat the background continuum accurately when computing coherent resonance line wings. This means that the usefulness of these wings as thermal diagnostics is severely compromised. The above considerations apply to the absorption part of the continuum term; in supergiants there is also a much stronger scattering part which does not play a role in the raising of wing intensities.

V. THE WILSON-BAPPU EFFECT IN SUPERGIANTS

I now use the results of the last three sections to discuss the factors involved in the formation of the emission width of a self-reversed chromospheric resonance line profile under conditions of strong coherency

in the line wings. These conditions can arise naturally as a result of the lower gravity in supergiants which leads to lower densities and thereby to less collisional redistribution.

I begin by taking a schematic solar-type chromosphere and then modifying it by changing the turbulent velocities, distribution of temperature versus mass column density, and the gravity. For this Paper I use $\Delta\lambda(k_1)$ to define the emission width W . The model atom I adopt is again for Mg II, and the line profiles are calculated using the same methods employed in realistic model chromosphere calculations (cf. Basri *et al.* 1979), using the correct redistribution weights; the only schematic part is the $T(M_R = M - M_0)$ distributions and the use of $r_0 = 10^{-9}$ for all computations. The model used for the solar case (model A) is shown in Figure 7a; the adopted gravity was $2 \times 10^4 \text{ cm s}^{-2}$ and solar abundances were assumed. Ionization and ground level populations are all assumed to be LTE; this approximation is sufficiently accurate for my purposes.

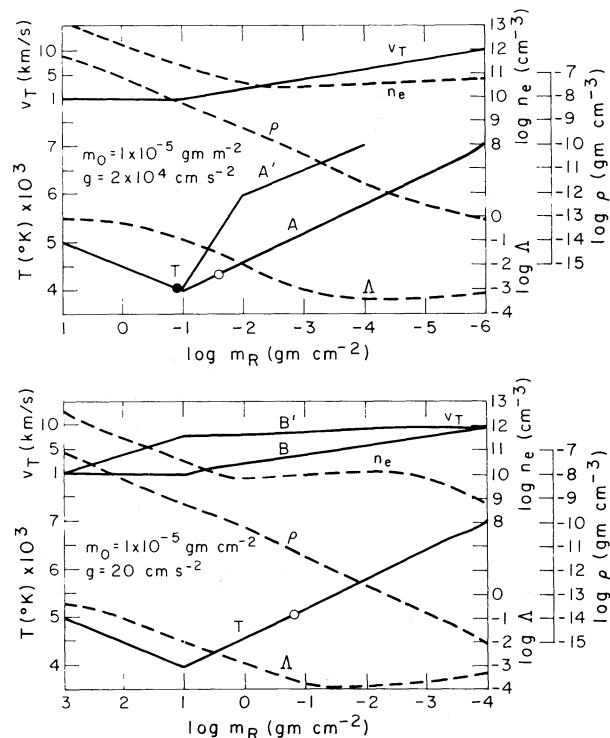


FIG. 5.—Chromospheric models of § V. Upper portion is the “solar” case, A, showing T , n_e , v_T , and Δ for this model. Cases A and A' were also run for $g = 20 \text{ cm s}^{-2}$; only T and v_T are appropriate to these cases. The open and filled circles on the temperature curves indicate $\tau(\Delta\lambda = W) = 1$ for cases A and A', respectively. Lower portion shows the supergiant case, B. Note that the model has been moved inward in m_R , partially offsetting the effect of the reduced gravity.

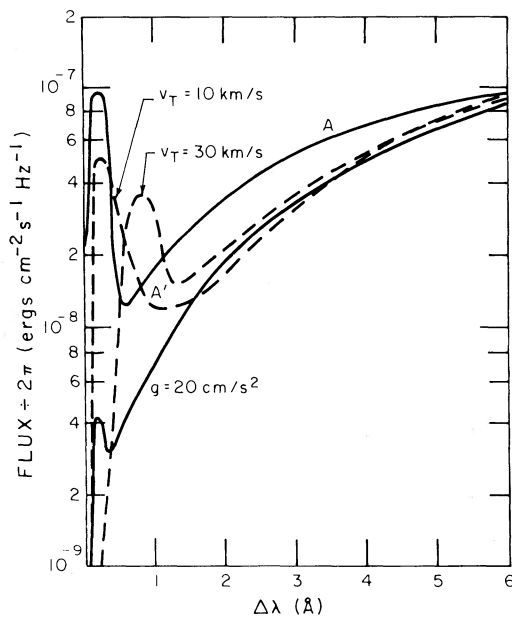


FIG. 6a

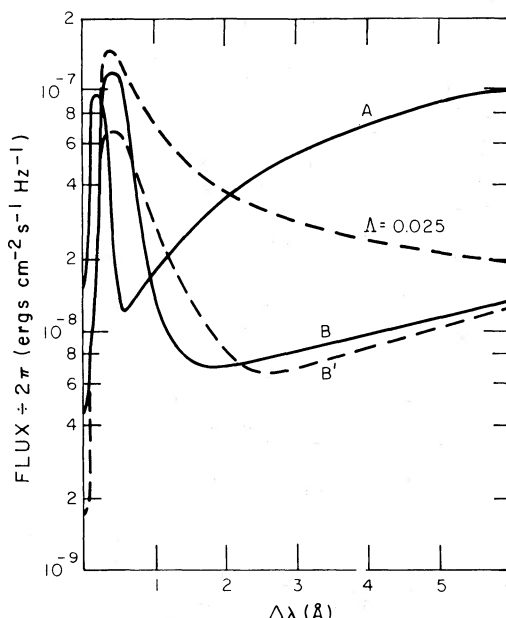


FIG. 6b

FIG. 6.—(a) *Solid lines*, emergent profiles for the temperature structure of case A, with both values of g . *Dashed lines*, emergent profiles for cases A' with $g=20$ and gradients of the microturbulent velocity from 1 to 10 and 30 km s^{-1} . (b) *Solid lines*, flux profiles for case A (same as 6a) and B. *Dashed lines*, profiles for case B with Δ increased to 0.025 and for case B' (different v_T distribution).

The main non-LTE effect on Mg II would be to stretch the optical depth scale at the top of the atmosphere because of overpopulation of the ground state, which is not an important effect for these schematic models. I used a microturbulent velocity distribution ranging from 1 to 10 km s^{-1} (Fig. 5a). Shown in Figure 6a is the emergent line profile for model A, with $W \approx 0.5 \text{ \AA}$ and a generally solar appearance. The effects of reducing the gravity to $2 \times 10^1 \text{ cm s}^{-2}$ are also shown; this reduces the incoherence fraction by almost two orders of magnitude. The source function is therefore decoupled from the chromospheric temperature rise deeper in the atmosphere, reducing the intensities in the line core and the contrast of the emission feature.

It is clear that some change in $T(M_R)$ is required to produce a profile resembling observations, which for a star of this gravity and solar spectral type have a similar appearance to the solar case except that W is increased to 2.5 \AA , and the wings are flatter (see Fig. 7). According to Ayres (1979) the change should be to move the temperature minimum to greater mass column density, but to examine other possibilities first I kept the same mass grid and increased the temperature gradient in the chromosphere, as in model A' (Fig. 5a). To further increase W , I raised the microturbulent velocities in the atmosphere as required by the classical explanation of the Wilson-Bappu effect (e.g., Scharmer 1976). The results for $v_T = 10$ and 30 km s^{-1} are shown in Figure 6a. The central reversal is too deep, as expected for this gravity (though turbulence on larger scales could fill this in), but—more to the point— W is

still only 1.5 \AA even with $v_T = 30 \text{ km s}^{-1}$ throughout the atmosphere. This is highly supersonic turbulence, and obviously still greater velocities would be required to increase W to its observed value. Furthermore, the contrast in the emission peak is diminished at higher velocities. I also ran a test with a microvelocity gradient from 3 to 30 km s^{-1} ; the results were similar to the 10 km s^{-1} case except that W was close to the 30 km

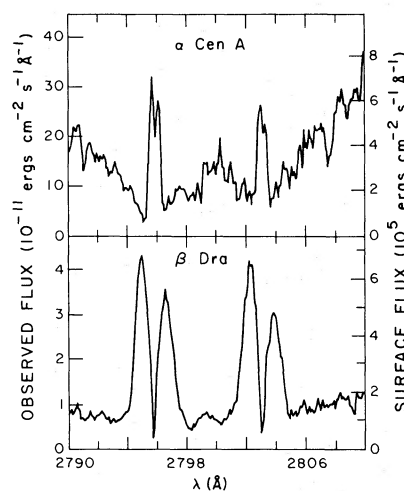


FIG. 7.—Observed profiles of Mg II for α Cen A (G2 V) and β Dra (G2 II) showing the effect of luminosity class on stars of the same spectral type. Note the wider emission peaks and shallower wings on the more luminous star.

s^{-1} result. I conclude that *turbulence by itself is not a viable explanation of the Wilson-Bappu effect in supergiants.*

I next followed the suggestion of Ayres and moved the whole atmosphere inward to greater mass column density. His scaling law has $m^* = m(T_{\min}) \sim g^{-1/2}$, so the masses everywhere should be increased by a factor 30. I used instead a factor of 100; this should produce a W that is too large if the assumptions used to derive the scaling law are valid. As we have seen in an earlier section, however, the Eddington-Barbier type relation between the minimum feature and the temperature minimum used to derive this scaling law does not hold for very coherent cases. Figure 6*b* shows the emergent profile for model A in the low gravity case moved inward by 100 times in mass column densities (model B, Fig. 5*b*). W is only increased to 1.5 Å and will remain at this value or less, independent of the value of m^* because the minimum feature is decoupled from the temperature structure. This is best illustrated by increasing the incoherence fraction arbitrarily to 0.025, the value appropriate for the Ca II K line. The result is shown in Figure 6*b*; now W is 6 Å as would be expected from finding the point in the wing where $\tau_r = 1$ at the temperature minimum.

One possibility is, of course, that the incoherence fraction is not correctly treated; I examine this in the next section. Changes in the background continuum opacity and source function affect the intensity at k_1 and in the wings, but have little effect on W . Otherwise it seems for this model that neither theory can yield a correct value of W for this gravity. A special combination of the theories works nicely; the correct value for W is obtained in model B' (Fig. 5*b*) if turbulent velocities of 8 km s $^{-1}$ are allowed to penetrate close to the temperature minimum, as shown in Figure 6*b*. These velocities are just barely supersonic, and so are more easily justified than those required without the increase in m^* . The line wings are flatter than for the solar case, which also agrees with observations (see Fig. 7).

The particular m^* chosen for model B' is not required to match W to observations; it could be decreased to Ayres's suggested value without affecting W because of the decoupling. In this case, however, decreasing m^* by a factor of 10 was sufficient to markedly lower the emission peak, indicating that the lower chromospheric temperature gradient would have to be steeper than in model B. The temperature gradient can influence the emission width if it is steep enough, because Doppler diffusion from a very bright feature can extend the emission feature further into the wings. In realistic atmospheres a steeper gradient can also mean that higher temperatures occur where the incoherence fraction is greater, further enhancing their effect. In practice, one is also constrained by the requirement of matching the Ca II K observations; this

line is somewhat optically thinner and has a lower bound to its incoherence fraction that is much greater than for Mg II, as discussed in the next section. Extensive modeling efforts with real data (Basri 1979) showed that these differences tend to provide enough constraints so a model that matches both lines is fairly unique. Calculation of the Ca II K profile for model A yielded a profile that only has a change in slope where the emission feature should be (the solar feature is very weak), but model B' yields a profile with the appropriate value for W and reasonable contrast between K_2 and K_3 (similar to β Dra).

VI. THE INCOHERENCE FRACTION

The results of the previous sections show that the correct treatment of the atomic processes which can redistribute line photons is important when using resonance line diagnostics in low-density atmospheres. There are three mechanisms through which an atom excited from a sharp level can reemit the photon at a different frequency in the atom's rest frame: an electromagnetic field perturbation, an almost elastic collision with a particle, or reprocessing through an intermediate transition. The first process can be induced by the passage of plasma waves (but they have to be very strongly nonthermal to have a significant effect) or by a close encounter with a charged particle. We shall lump the latter with elastic collisions under the general term "collisions" and ignore the former. The last process refers to the population of the given level by emission or absorption of photons from levels other than the ground state.

For Ca II and Mg II the electron Stark broadening and van der Waals broadening are the dominant contributors to the collisional line width. For these species the impact regime extends to several angstroms, so the broadening parameters are almost independent of wavelength. The theoretical calculations for the Stark damping parameter are fairly well in hand and agree with experiment to within a factor of 2 (Raymer 1979). Stark broadening is the dominant source of collisional redistribution in supergiants. I adopted values of $1.6 \times 10^{-6} n_e$ and $2.6 \times 10^{-6} n_e$ for the Mg II and Ca II Stark parameters (Shine 1975*b*). The van der Waals parameters are less well understood; Ayres (1977) has used solar models to calibrate the Ca II parameter, but theory brackets his value by an order of magnitude on either side. Fortunately, this is not the dominant term for either Ca II or Mg II in supergiants, and would have to be raised by almost two orders of magnitude to make a difference. Collisional rates between the 4^2P states are also relatively small.

By simple analysis, such as in Ayres (1975), it can be shown that the effect of other levels is just what one would expect from simple physical reasoning. His results show that for a metastable level m below the

upper level of the transition u to g , the modified incoherence fraction will have a lower bound for low densities of

$$\Lambda' \geq \frac{a}{1+a}, a \equiv \frac{A_{um}}{A_{ug}},$$

the ratio of Einstein A -values. Using essentially the same formulation to study the effect of a transition to a higher-lying level h , I find the lower bound to be

$$\Lambda' \geq \frac{a'}{n_u/n_h + a'}, a' \equiv \frac{A_{hu}}{A_{ug}},$$

for LTE. Thus if a' is close to unity and $n_u \gg n_h$, the lower bound will just be the ratio of the populations of the two levels n_h/n_u . At most the wings of the given line will be populated by other lines at the LTE rates with the wavelength dependence of the absorption profile. The term "modified" is applied to this incoherence fraction because it is really an expression of an external source term for line wing photons rather than a true reshuffling of energy states within the upper level. It has the same eventual effect, however.

In Ca II, for example, there are metastable (3^2D) levels lying below the excited state for the K line. The likelihood of the excited atom branching to one of these rather than returning a photon in the K line is given by the ratio of Einstein A -coefficients for the two transitions. This probability is much higher than for collisional reshuffling through most of the supergiant atmosphere and so provides a lower bound to the incoherence fraction. Excitations from the metastable level proceed at a rate given by the product of the absorption profile and the radiation field in the infrared triplet lines. In typical models this radiation field is only one-half of its Planckian value in supergiants at the level where the K line wings are formed because the infrared transitions are optically thin there. The modified incoherence fraction is thus $\Lambda' = (A_{\text{infrared}}/A_{\text{K line}}) (J_\nu/B_\nu)_{\text{infrared}} \sim 0.03$, and should not fall much below this value. Eventually, as one moves deeper into the atmosphere the density increases sufficiently for collisional redistribution to rise above this value.

In Mg II there are no levels between the 3^2P states and the ground state. The lower bound to the incoherence fraction provided by other levels must therefore come from the next level above, whose population will be much less because of its higher energy. In Mg II this 3^2D level happens to lie above the 3^2P levels as far as they are above the ground state. Thus this line occurs in the wing of the K line and the radiation field at the wavelength is increased as a result of the greater opacity (compared to what it would be without the K line). Since the radiation fields for the two transitions are similar, the branching ratio is basically governed by the relative rates out of the 3^2P states for the two

transitions. In LTE this ratio is the Boltzmann factor for a transition at $\lambda 2800$, and so is of order 10^{-4} for the temperatures in the chromosphere. Because the collisional rates are even less than this in supergiant chromospheres, the modified incoherence fraction tends to drop to this value for Mg II k , implying strong coherence in the wings compared to Ca II K. Higher-lying levels will contribute even less to the wing source functions, as will continuum transitions, because of the smaller populations of these levels.

It seems, therefore, that the amount of redistribution that occurs for strong resonance lines in supergiants attains rates in the chromosphere which are bounded at the low end by radiative reprocessing from other levels. Lower in the photosphere, collisions again become important. I note that the gravity and densities chosen for illustration here are at the high end for supergiants; in most of these stars the collisional rates will generally be even less important. The real test comes, of course, in attempts to match observations in several lines such as Ca II K, Mg II k , and weaker lines such as $\lambda 8542$ (Ca II) or upper level transitions like H α with one model chromosphere. We should recognize, however, that one-component models are only a very crude approximation to the dynamic, inhomogeneous conditions likely to exist in the chromospheres of these stars.

VII. SUMMARY

The formation of chromospheric emission features in low-density atmospheres is strongly influenced by the effects of partial frequency redistribution of resonance line photons. Coupling to the local Planck function will be greatest near line center where the optical depth is greatest and far in the wings where the background continuum exerts control. In between, the wing source functions will tend to a coherent scattering form, so there is a natural tendency for an emission peak and minimum feature to appear in line profile, even for an isothermal atmosphere. The more coherent the line formation problem is, the more these factors will determine the line profile and the less this profile will reflect the temperature structure of the chromosphere. The minimum feature can be many Doppler widths from line center, so Doppler velocities may not be responsible for the emission peak width. These velocities can have some influence, however, because of Doppler diffusion of core photons into the wings. This diffusion is important in more coherent cases, so that use of the Kneer approximation for the partial redistribution weights is invalid for many stellar applications. The scale of the motions involved need not be "microturbulent"; fairly large scale organized motions of modest amplitude also yield broad symmetric profiles which have the additional advantage that the shallower central reversals more closely resemble observations. Treatment of the background continuum

must be done with care, even for strong lines, because of the coherence of the wings.

The above points have an obvious bearing on the interpretation of line profiles for chromospheric models and on possible explanations of the Wilson-Bappu effect. In the case of supergiants, they reduce the usefulness of resonance line diagnostics for deriving temperature structures, making it important to use as many different diagnostics as possible when building a model chromosphere. At the same time they suggest a reexamination of the Wilson-Bappu effect in supergiants. These stars have a disproportionate influence on the derived slope of the relation, yet the coupling of the emission width to the temperature structure of the star may be small for these cases, and fewer independent determinations of their absolute luminosity are available. The Doppler explanation for the Wilson-Bappu effect is certainly not the predominant one. The variation of the position of the temperature minimum in mass column density with gravity is derived by Ayres

(1979) using oversimplified assumptions, but it seems likely that this is the primary qualitative reason for the Wilson-Bappu effect, over the broad range of luminosities it covers. There are many factors that can influence the emission width, however, so future work on this remarkable effect should study the details of line formation more closely.

This work is supported by the National Aeronautics and Space Administration under grants NAS5-23274 and NGL-06-003-057 to the University of Colorado. I gratefully acknowledge the support of the National Center for Atmospheric Research which granted the computer time used in this project. I would like to acknowledge the help of Dr. Richard Shine, both in supplying the original version of the computer code used, and for his many helpful comments on this paper. I would also like to thank Dr. Jeffrey Linsky for his encouragement and advice during this project.

REFERENCES

- Ayres, T. R. 1975, *Ap. J.*, **201**, 799.
 ———. 1977, *Ap. J.*, **213**, 296.
 ———. 1979, *Ap. J.*, **228**, 509.
 Ayres, T. R., and Linsky, J. L. 1976, *Ap. J.*, **205**, 874.
 Baliunas, S. L., Avrett, E. H., Hartmann, L. W., and Dupree, A. K. 1979, *Ap. J. (Letters)*, **233**, L129.
 Basri, G. S. 1979, Ph.D. thesis, University of Colorado.
 Basri, G. S., Linsky, J. L., Bartoe, J.-D. F., Brueckner, G. E., and van Hoosier, M. C. 1979, *Ap. J.*, **230**, 924.
 Carlsten, J. L., Szöke, A., and Raymer, M. G. 1977, *Phys. Rev. A*, **15**, 1029.
 Chiu, H. Y., Adams, P. S., Linsky, J. L., Basri, G. S., Maran, S. P., and Hobbs, R. W. 1977, *Ap. J.*, **211**, 453.
 Frisch, H. 1979, SAO preprint.
 Frisch, U., and Frisch, H. 1976, *M.N.R.A.S.*, **175**, 157.
 Gail, H.-P., Sedlmayr, E., and Traving, G. 1975, *Astr. Ap.*, **44**, 421.
 Hummer, D. G. 1962, *M.N.R.A.S.*, **125**, 21.
 ———. 1969, *M.N.R.A.S.*, **145**, 95.
 Jeffries, J. T., and White, O. R. 1960, *Ap. J.*, **132**, 767.
 Kelch, W. L., Linsky, J. L., Basri, G. S., Chiu, H. Y., Chang, S., Maran, S. P., and Furenlid, I. 1978, *Ap. J.*, **220**, 962.
 Kneer, F. 1975, *Ap. J.*, **200**, 975.
 Magnan, C. 1974, *Astr. Ap.*, **35**, 233.
 Mihalas, D. 1978, *Stellar Atmospheres* (2d ed.; San Francisco: Freeman).
 Mihalas, D., Shine, R. A., Kunasz, P. B., and Hummer, D. G. 1976, *Ap. J.*, **205**, 492.
 Milkey, R. W., and Mihalas, D. 1973, *Ap. J.*, **185**, 709.
 Omont, A., Smith, E. W., and Cooper, J. 1972, *Ap. J.*, **175**, 185.
 Raymer, M. 1979, Ph.D. thesis, University of Colorado.
 Rutten, R. J., and Milkey, R. W. 1979, *Ap. J.*, **231**, 277.
 Scharmer, G. B. 1976, *Astr. Ap.*, **53**, 341.
 Shine, R. A. 1975a, *Ap. J.*, **202**, 543.
 ———. 1975b, Ph.D. thesis, University of Colorado.
 Shine, R. A., Milkey, R. W., and Mihalas, D. 1975, *Ap. J.*, **201**, 222.
 Vardavas, I. M. 1976, *J. Quant. Spectrosc. Rad. Transf.*, **16**, 715.
 Vardavas, I. M., and Cannon, C. J. 1976, *Astr. Ap.*, **53**, 107.
 Vernazza, J. E., Avrett, E. H., and Loeser, R. 1973, *Ap. J.*, **184**, 605.

G. BASRI: Space Sciences Laboratory, University of California, Berkeley, CA 94720